Supplement of Biogeosciences, 21, 3985–4005, 2024
https://doi.org/10.5194/bg-21-3985-2024-supplement

Biogeosciences Open Access EGU

Supplement of

Evolution of oxygen and stratification and their relationship in the North Pacific Ocean in CMIP6 Earth system models

Lyuba Novi et al.

Correspondence to: Lyuba Novi (lnovi3@gatech.edu)

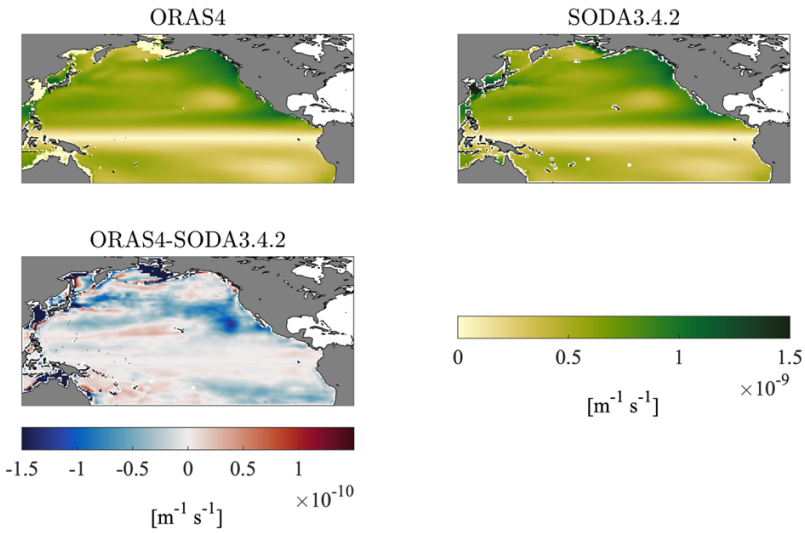

Fig. S1: Comparison of IPV* 1988-2014 climatology computed using ORAS4 and SODA.3.4.2.

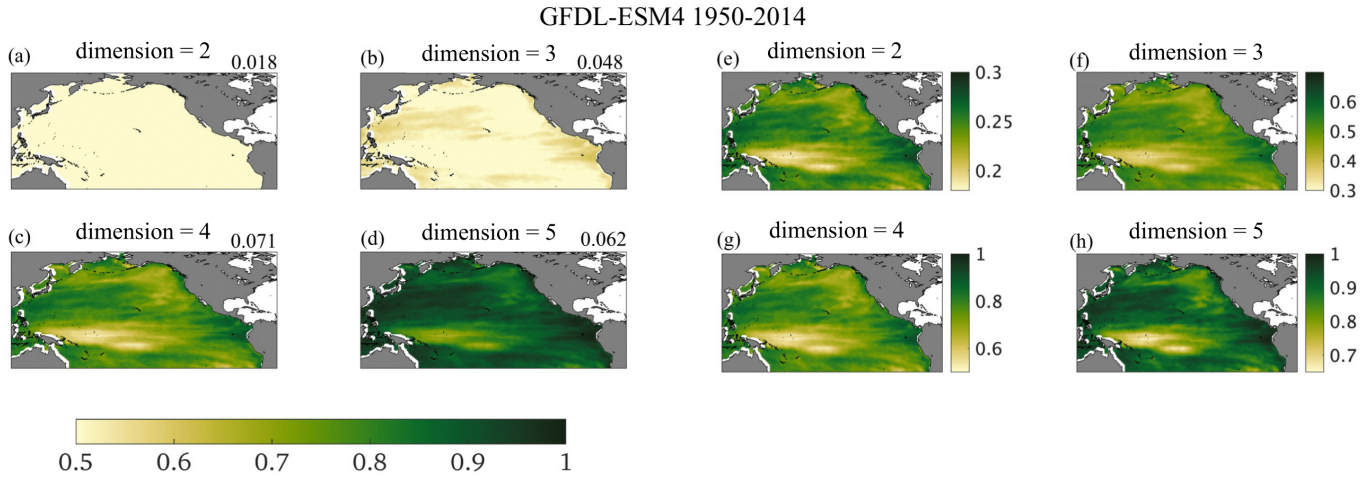

Fig. S2. Historical (1950-2014) GFDL-ESM4 IPV* (Information) Entropy (IE) maps for microstates of dimension 1, 2, 3 and 4. Panels (a)-(d) use the same color scale as the main text. Each panel from (e)-(h) (the same fields as in panels (a)-(d)) has a different color scale, to highlight the similarities across spatial patterns.

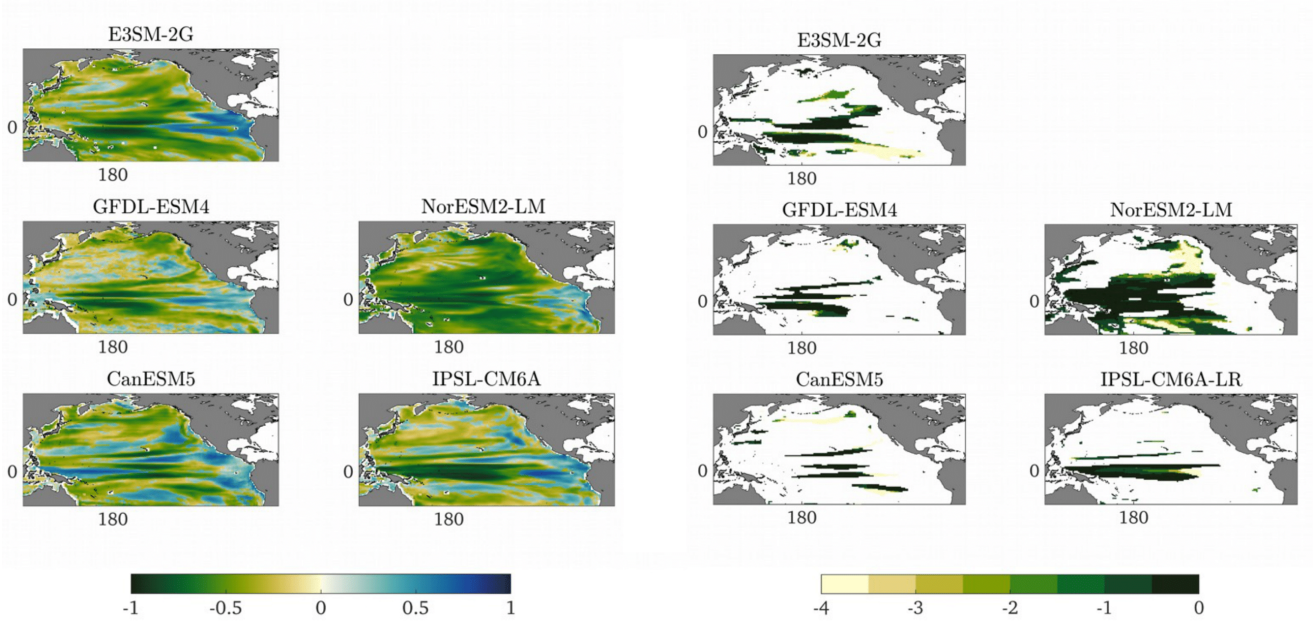

Fig. S3. Left: 1950-2014 (1960-2014 for E3SM-2G) maximum absolute correlation (c.c) at any lag, between O_2 anomalies and IPV* anomalies (full fields, i.e. not residuals). Right: Corresponding lags (months) shown only in grid points where c.c $\leq$ - 0.5 and corresponding lag $\leq$ 0. Negative lags mean IPV* preceding. Lags colorbar saturates at –4.

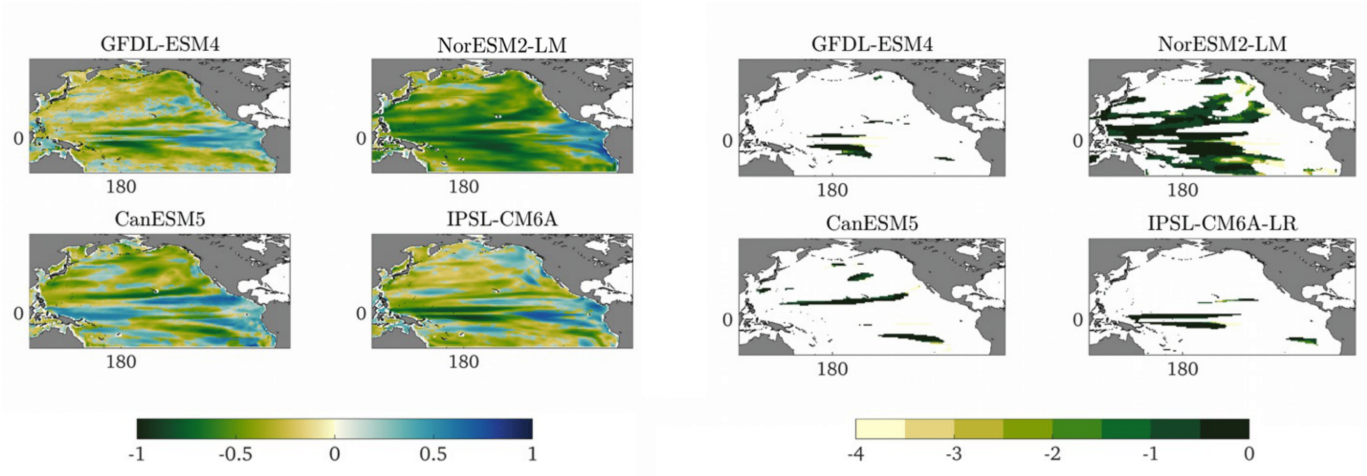

Fig. S4. As in Fig. S3 but for the future projections, 2036-2100.

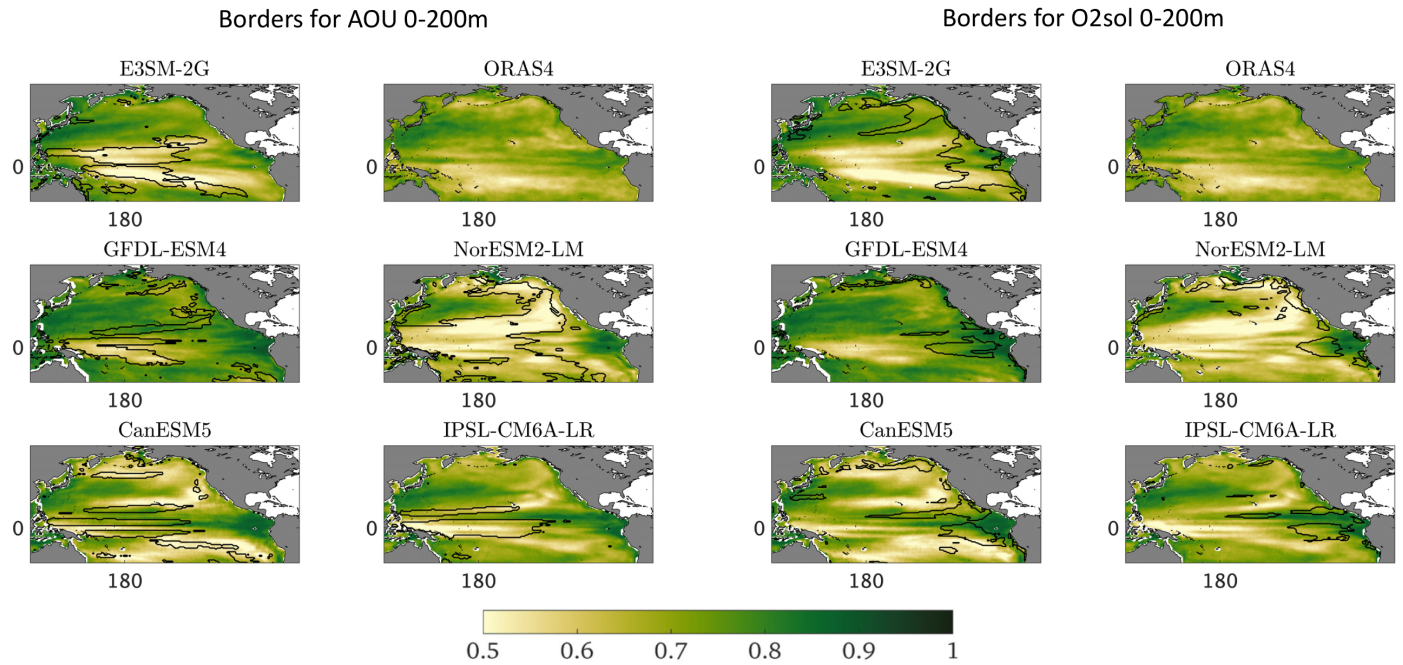

Fig. S5. The IPV* entropy field over 1950-2014 (CMIP6 historical period) for the ESMs, and over 1960-2014 in the ocean hindcast and ORAS4. The left panels show areas where IPV* and AOU time series are correlated with correlation coefficients ≥ 0.5 superimposed with black contours. The right panels show areas where IPV* and O_{2sol} time series are anticorrelated with correlation coefficients ≤ -0.5 also superimposed with black contours.

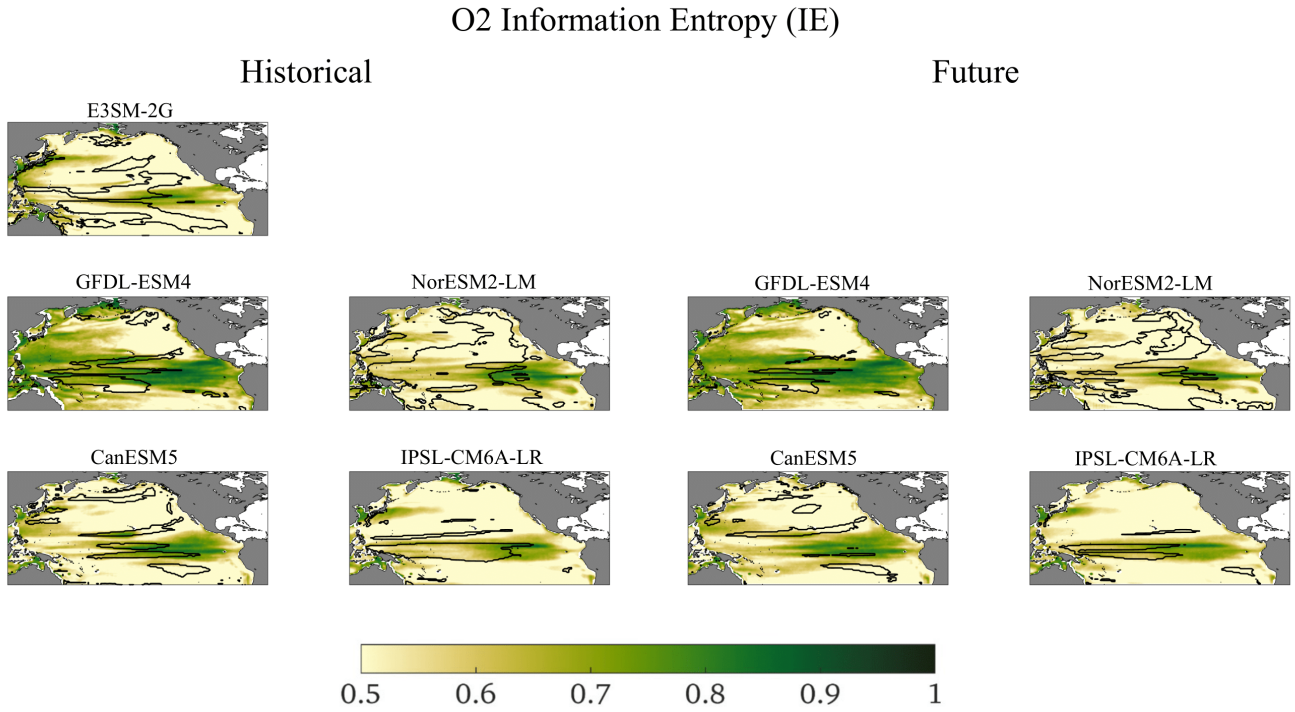

Fig. S6. O2 information entropy in the historical interval (left) and in the future (right) for the ESMs, and in the historical 1960-2014 period for the hindcast, with superposed the contours of the areas where IPV* and O_2 time series are anticorrelated with correlation coefficients $\leq$ -0.5

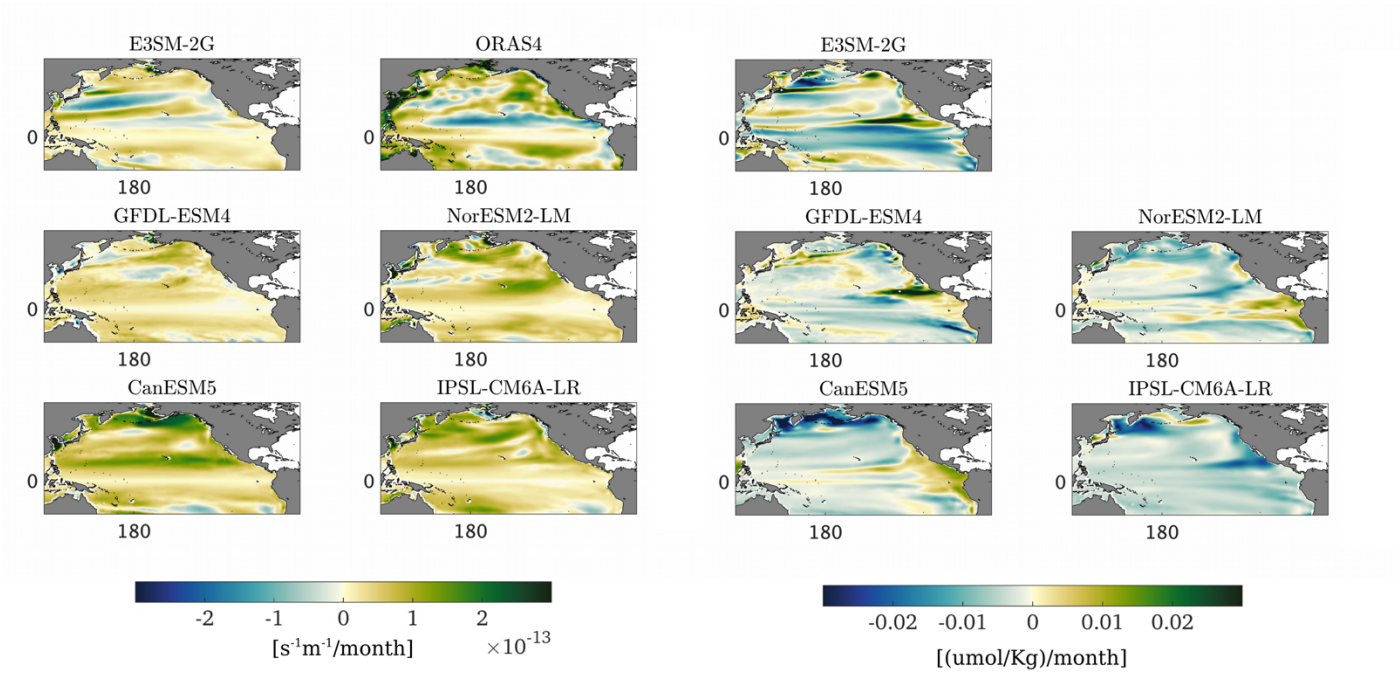

Fig. S7. Linear trend of residual IPV^*_{res} (left) and residual O_{2res}(right) from 1950 to 2014 (1960 to 2014

for ORAS4 and E3SM-2G). Seasonal cycles have been removed before calculating linear trend. Color scales saturate at +/- 3 10^{-13} (IPV^*_{res}) and +/- 0.03 (O_{2res}).

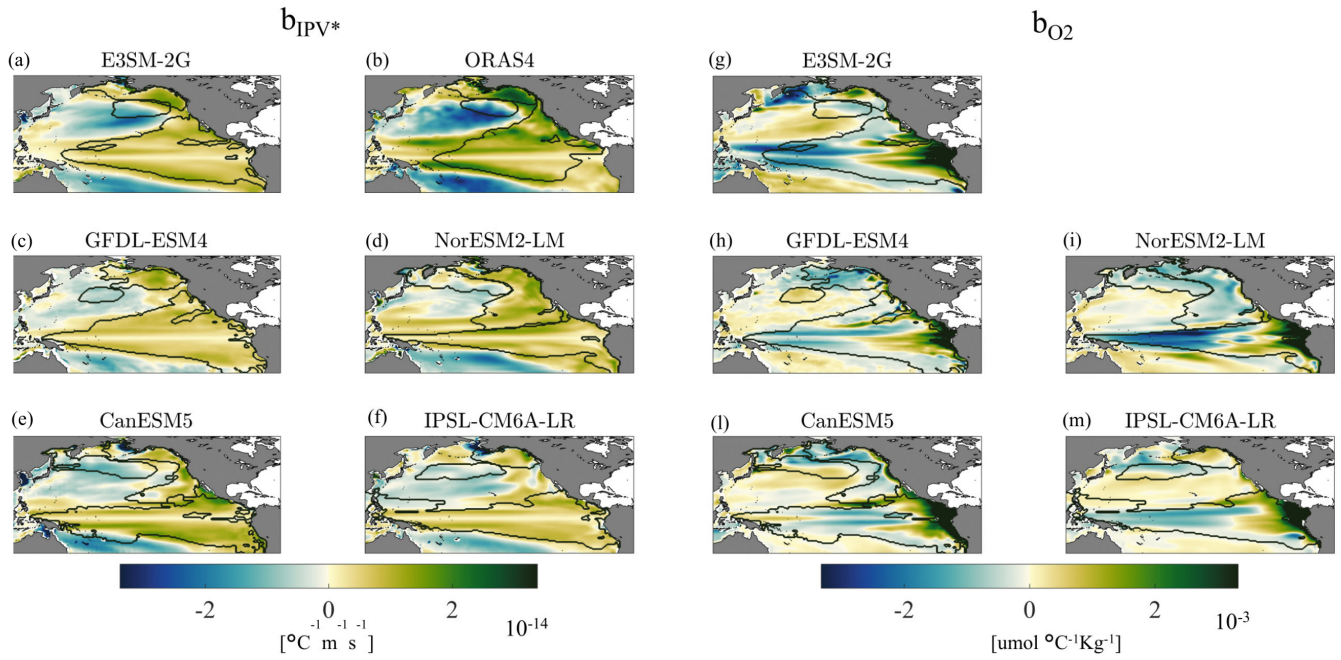

Fig. S8. ENSO-regression coefficient (b_{IPV}* (left) and b_{O2} (right)) maps for the historical period. Black contours are the ENSO and the PDO+ and PDO- domains computed through δ-MAPS. Color limits are fixed as +/- 3 standard deviations of the ensemble for each variable over the whole area.

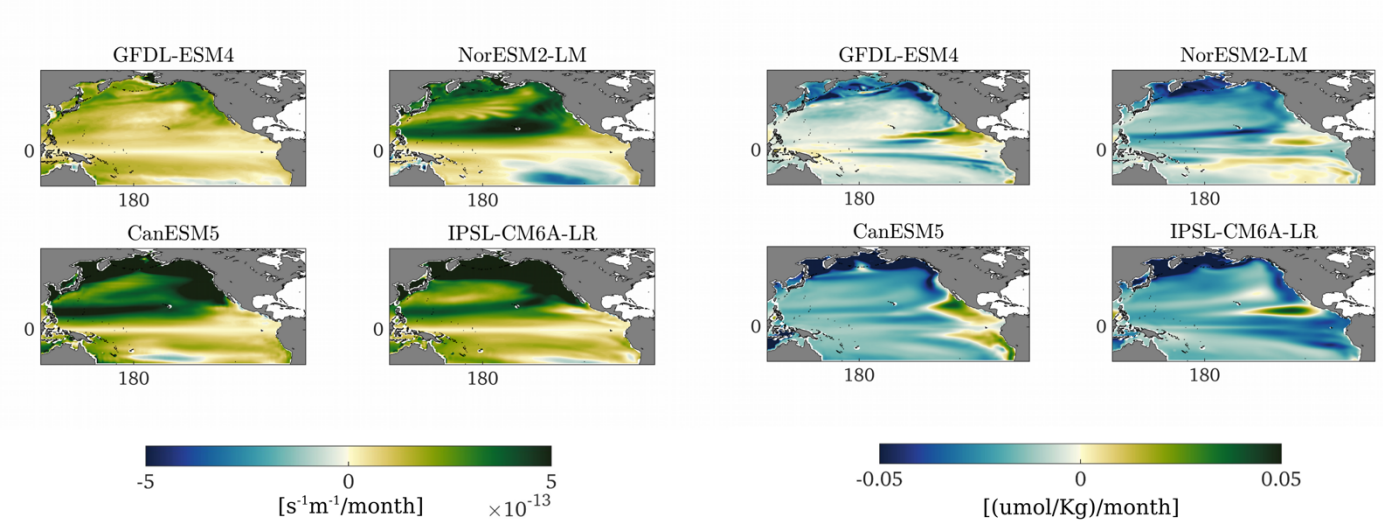

Fig. S9. The same as in Fig. S7 but for future projection from 2036 to 2100. Color scales saturate at +/- 5 10^{-13} (IPV^*_{res}) and +/- 0.05 (O_{2res}).

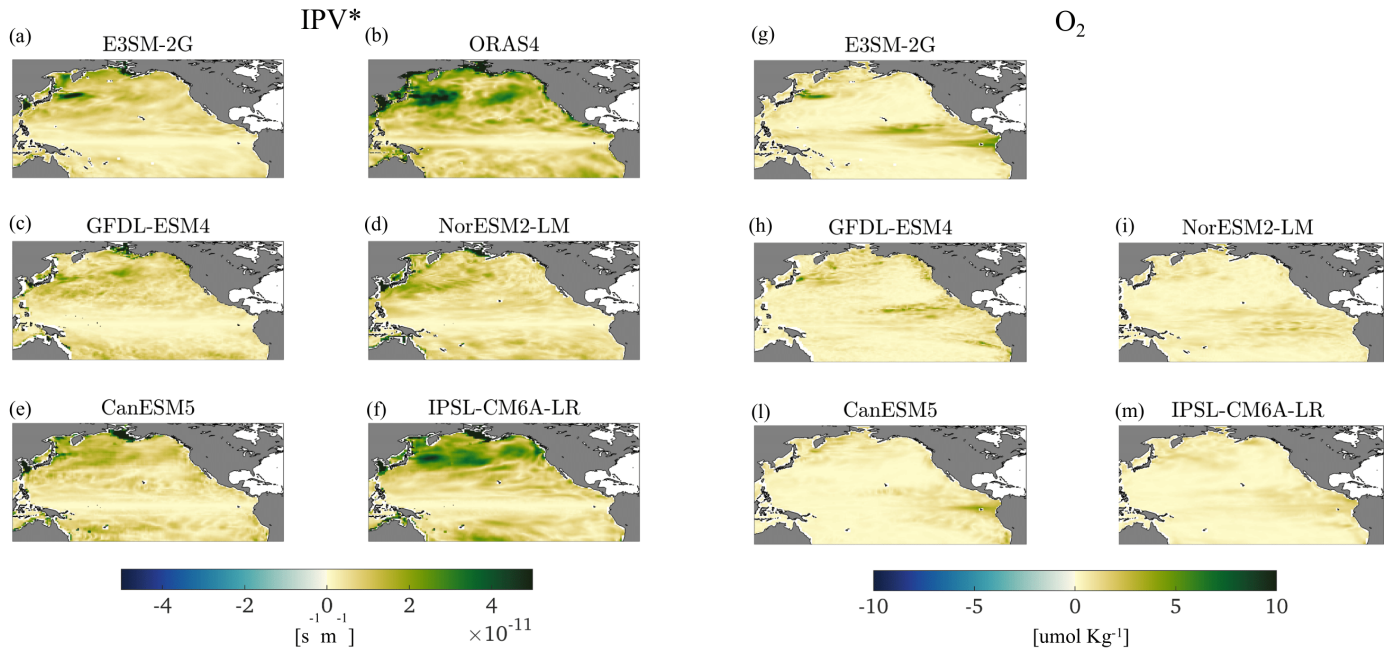

Fig. S10. Seasonal standard deviation (i.e. standard deviation among 4 seasonal maps per each panel) of Δ_{means} for the historical period, 1950-2014 (1960-2014 for ORAS5 and E3SM-2G).

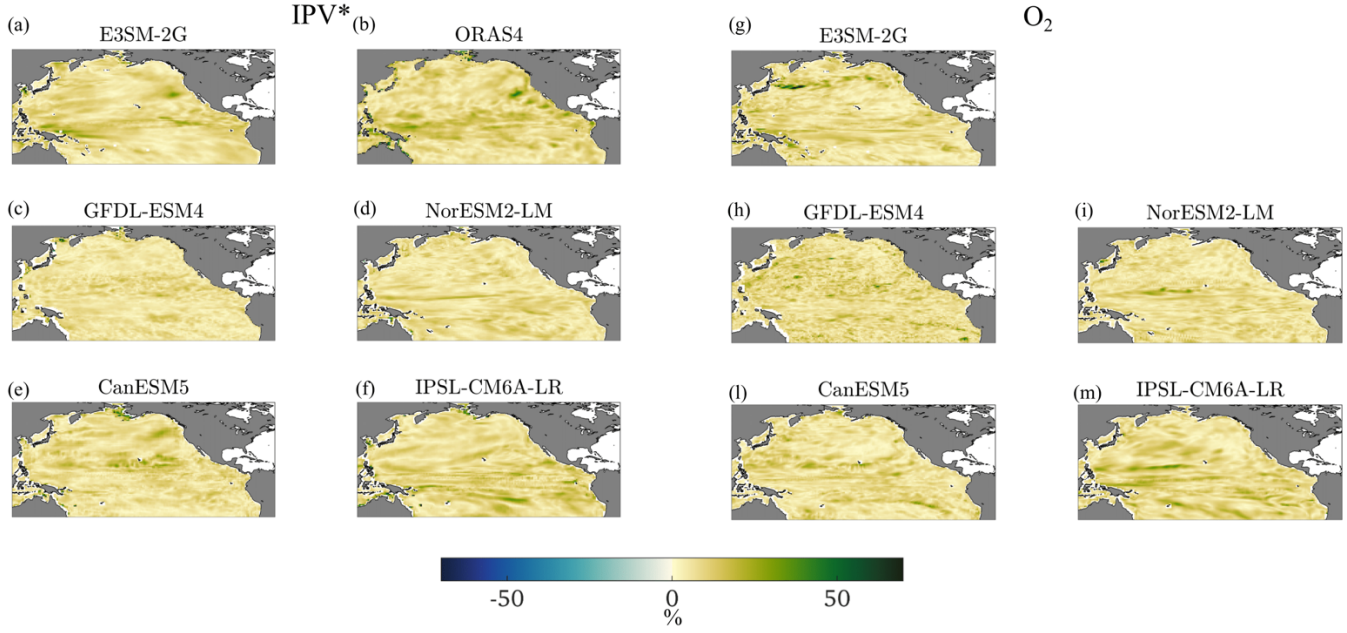

Fig. S11. As in Fig. S10 but for the seasonal standard deviation of $\Delta_{variability}$.

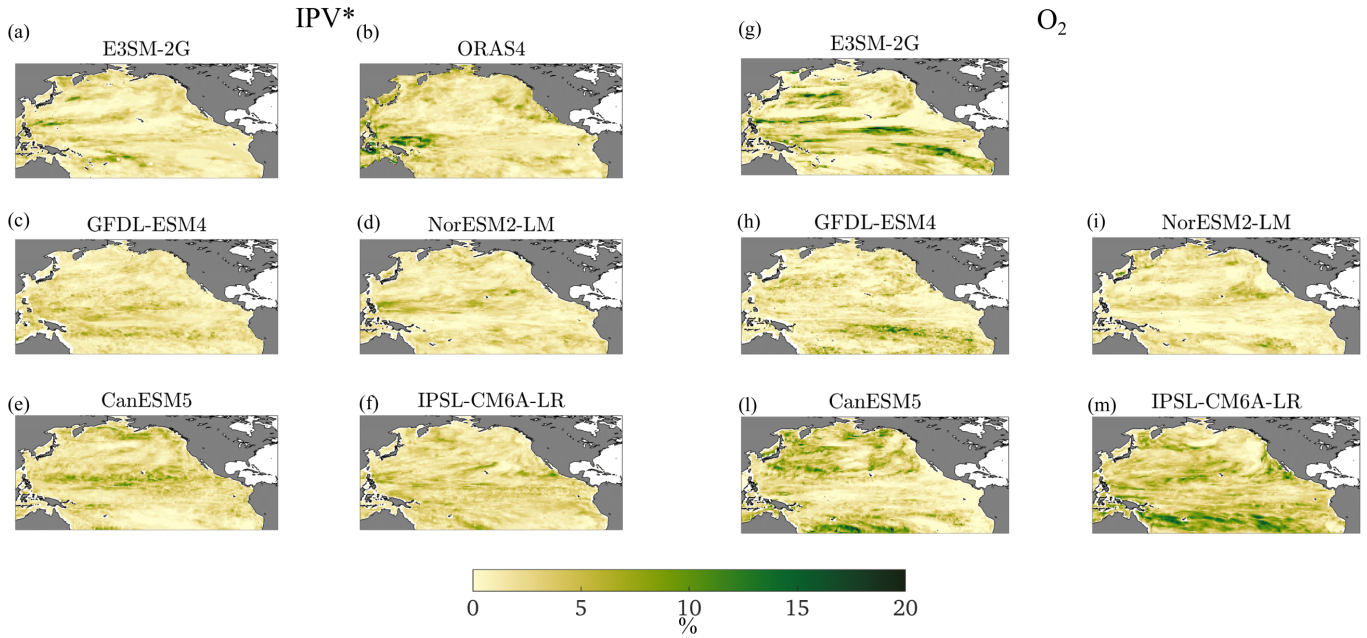

Fig. S12. As in Fig. S10 but for the seasonal standard deviation of Δ_{extremes}.

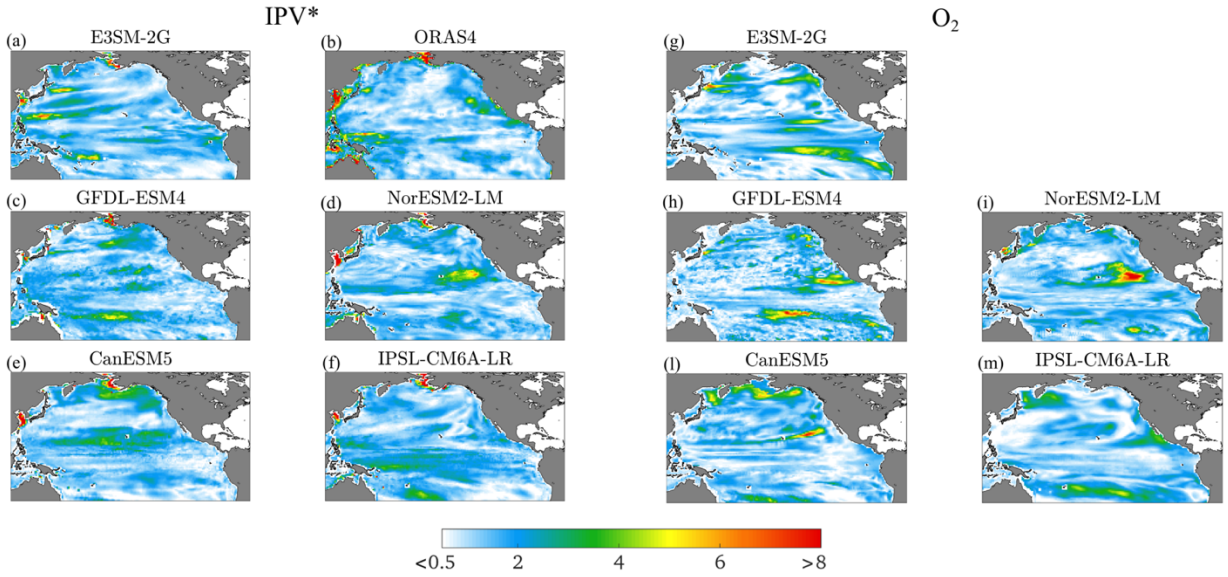

Figure S13. 1950-2014 SED *index* for residual IPV*$_{\text{res}}$ (left) and residual $O_{2\text{res}}$ (right). The color scale is produced with the rgbmap (Greene, 2023).

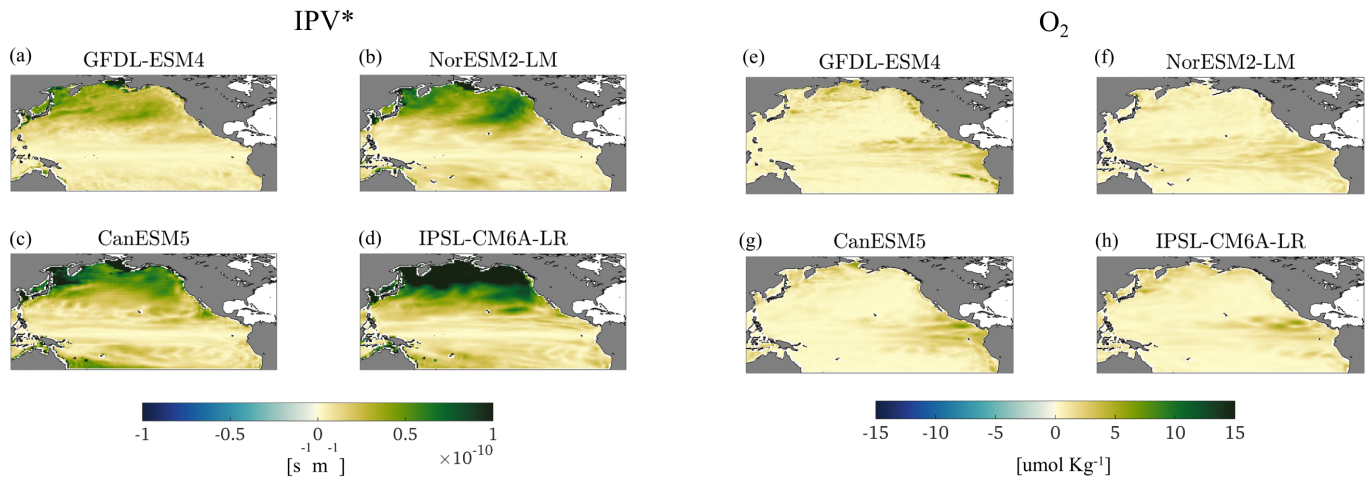

Fig. S14. Seasonal standard deviation (i.e. standard deviation among 4 seasonal maps per each panel) of Δ_{means} for the future projection period, 2036-2100.

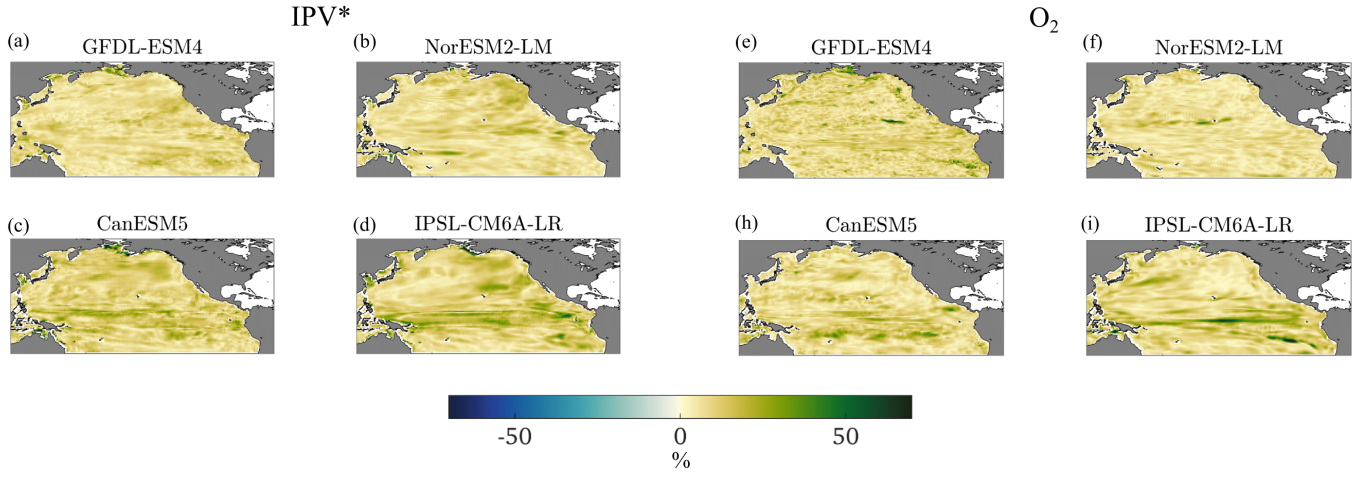

Fig. S15. As in Fig. S14 but for the seasonal standard deviation of $\Delta_{variability}$.

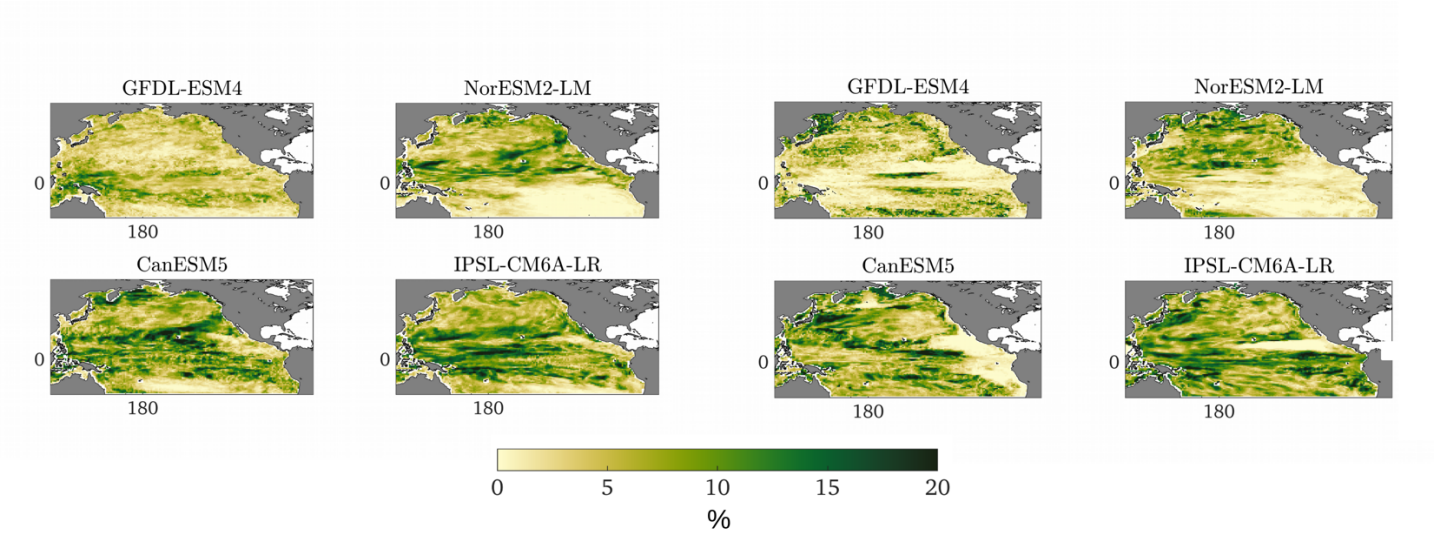

Fig. S16. As in Fig. S14 but for the seasonal standard deviation of $\Delta_{extremes}$.

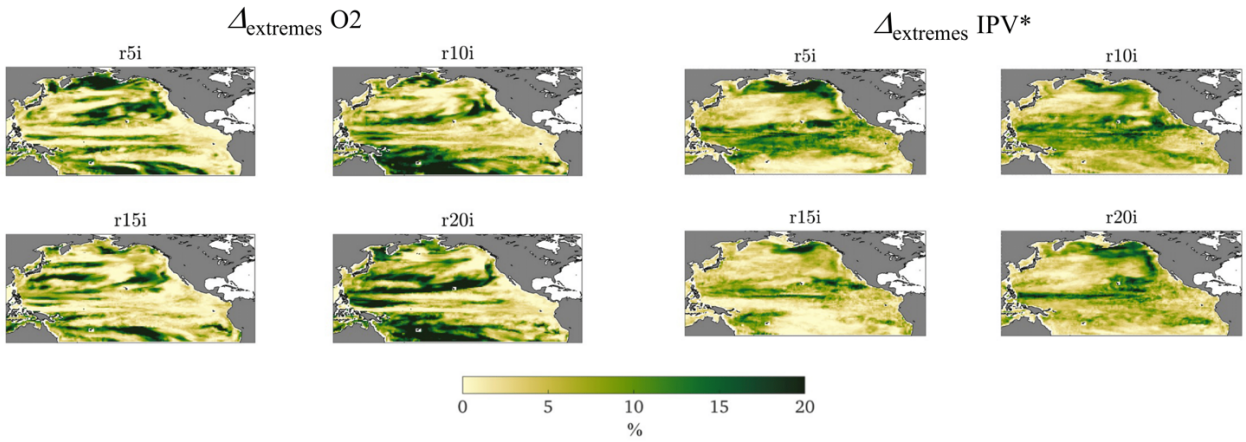

Figure S17. O_2 (left) and IPV*(right) indicators for changes in extremes (historical, whole signal) for four different ensemble members of the CanESM5 model.

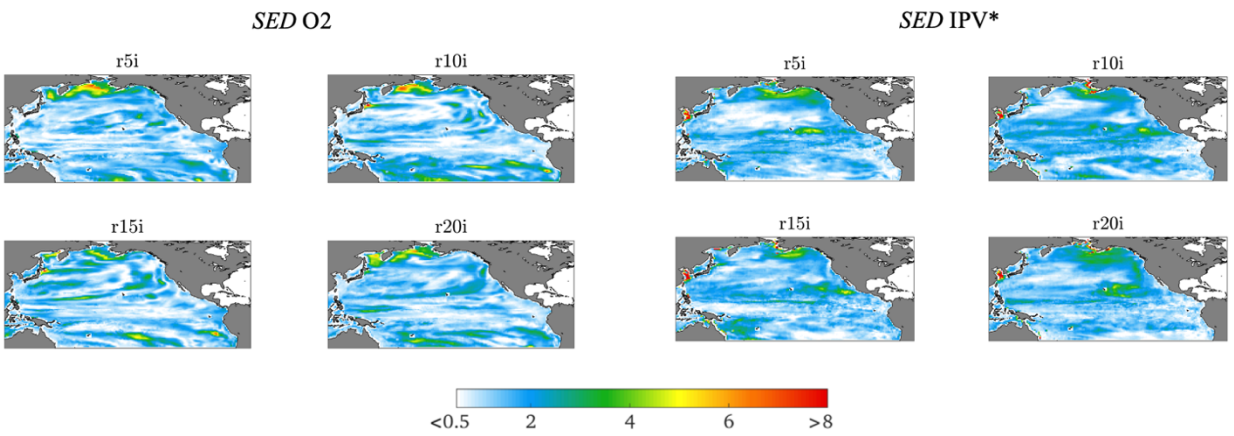

Figure S18. O_2 (left) and IPV*(right) SED indices (historical, whole signal) for four different ensemble members of the CanESM5 model.

Shuffling test for statistical significance of indicators spatial correlations

The significance of the correlation coefficient (c.c) reported in Table 2, Table 3, Fig. 4 and Fig. 5 in the Main Text is tested with a random shuffling test. Each indicator is a matrix with NaNs values over land points and non-NaNs values over the ocean points. Given each indicator is initially a matrix X, we set $\boldsymbol{N}$=10000 as the total number of shuffling cycles, and for each cycle n = 1, …, $\boldsymbol{N}$ we proceeded as described. We first shuffle (via random permutation) X's elements column by column and row by row. The resulting shuffled matrix Y does not distinguish between ocean and land points, and includes NaNs in random positions which may alter the final statistical significance test. To overcome this issue, we proceed as follows.
(i) We select only the ocean grid points from Y (populated with shuffled values and NaNs at random positions and again does not distinguish ocean from land), we put a numeric mask (-999.999) on the land, and store the result in a new matrix A;
(ii) Conversely, we select only the land points in the shuffled matrix (populated with shuffled values and NaNs at random positions and again does not distinguish ocean from land), we put NaNs on the ocean points, and store the result in a new matrix B (i.e. B has no-NaNs just on some random land points, and all NaNs elsewhere) ;
(iii) Next, we randomly replace only the no-NaNs of matrix B into the NaNs of matrix A. The resulting A has a mask (-999.999) on land points, and a random permutation of all the ocean points at ocean locations.
(iv) We finally replace the land-mask in A with NaNs and compute the field-correlations between the meaningful pairs of indicators ($\Delta_{means\ O2}$ with $\Delta_{means\ IPV*}$, $\Delta_{variability\ O2}$ with $\Delta_{variability\ IPV*}$ and $\Delta_{extremes\ O2}$ with $\Delta_{extremes\ IPV*}$), skipping NaNs values.

The resulting value represents the spatial correlation between (spatially) randomized indicators ($c.c._{shuffle}$). Finally, at each cycle, we compared $c.c._{shuffle}$ with the c.c. originally computed for the non-shuffled indicators, to measure how many times out of $\boldsymbol{N}$ we obtain "*by chance" (*i.e. for a random realization of the existing pixel values*)* a correlation stronger or equal to c.c. in absolute value, i.e. how many times *m* it

is $|c.c._{shuffle}| > |c.c.|$. The percentage $P = 100(m/\boldsymbol{N})$ gives a measure of the statistical significance of c.c., i.e. the corresponding c.c. is found "*by chance*" less of P% of the times. In this work, we assumed significant c.c. with $P \leq 5\%$.